AD

TECHNICAL REPORT BRL-TR-2785

SOME ASPECTS OF ADIABATIC SHEAR BANDS

THOMAS W. WRIGHT

MARCH 1987

US ARMY BALLISTIC RESEARCH LABORATORY
ABERDEEN PROVING GROUND, MARYLAND

Destroy this report when it is no longer needed.
Do not return it to the originator.

Additional copies of this report may be obtained from the National Technical Information Service, U. S. Department of Commerce, Springfield, Virginia 22161.

The findings in this report are not to be construed as an official Department of the Army position, unless so designated by other authorized documents.

The use of trade names or manufacturers' names in this report does not constitute indorsement of any commercial product.

UNCLASSIFIED
SECURITY CLASSIFICATION OF THIS PAGE

REPORT DOCUMENTATION PAGE

Form Approved
OMB No. 0704-0188
Exp. Date: Jun 30, 1986

1a. REPORT SECURITY CLASSIFICATION Unclassified	1b. RESTRICTIVE MARKINGS
2a. SECURITY CLASSIFICATION AUTHORITY	3. DISTRIBUTION / AVAILABILITY OF REPORT Approved for public release; distribution is unlimited.
2b. DECLASSIFICATION / DOWNGRADING SCHEDULE	
4. PERFORMING ORGANIZATION REPORT NUMBER(S)	5. MONITORING ORGANIZATION REPORT NUMBER(S)
6a. NAME OF PERFORMING ORGANIZATION Ballistic Research Laboratory 6b. OFFICE SYMBOL (*If applicable*) SLCBR-TB-S	7a. NAME OF MONITORING ORGANIZATION
6c. ADDRESS (*City, State, and ZIP Code*) Aberdeen Proving Ground, MD 21005-5066	7b. ADDRESS (*City, State, and ZIP Code*)
8a. NAME OF FUNDING / SPONSORING ORGANIZATION 8b. OFFICE SYMBOL (*If applicable*)	9. PROCUREMENT INSTRUMENT IDENTIFICATION NUMBER
8c. ADDRESS (*City, State, and ZIP Code*)	10. SOURCE OF FUNDING NUMBERS PROGRAM ELEMENT NO. / PROJECT NO. / TASK NO. / WORK UNIT ACCESSION NO

11. TITLE (*Include Security Classification*)
SOME ASPECTS OF ADIABATIC SHEAR BANDS

12. PERSONAL AUTHOR(S)
Wright, T. W.

13a. TYPE OF REPORT	13b. TIME COVERED	14. DATE OF REPORT (*Year, Month, Day*)	15. PAGE COUNT
Technical Report	FROM _____ TO _____		

16. SUPPLEMENTARY NOTATION

17. COSATI CODES		
FIELD	GROUP	SUB-GROUP
20	11	

18. SUBJECT TERMS (*Continue on reverse if necessary and identify by block number*)
shear bands microplasticity
high rate deformation

19. ABSTRACT (*Continue on reverse if necessary and identify by block number*)

A one-dimensional continuum formulation for the initiation and growth of adiabatic shear bands is reviewed, including some remarks on the underlying assumptions. A short description of some perturbation calculations introduces the idea of stress collapse and band formation as a bifurcation from homogeneous deformation, and an approach for estimating the critical time of collapse for infinitesimal perturbations is introduced. Steady solutions are exhibited and their interpretation as central boundary layers is suggested. Finally it is shown that in a certain limit shear bands occur following a hyperbolic to elliptic transition in the governing equation, and in a concluding remark dipolar plasticity is introduced as a possible alternative continuum description.

20. DISTRIBUTION / AVAILABILITY OF ABSTRACT	21. ABSTRACT SECURITY CLASSIFICATION
☒ UNCLASSIFIED/UNLIMITED ☐ SAME AS RPT. ☐ DTIC USERS	Unclassified
22a. NAME OF RESPONSIBLE INDIVIDUAL Wright, T. W.	22b. TELEPHONE (*Include Area Code*) 301-278-6046 22c. OFFICE SYMBOL SLCBR-TB-S

DD FORM 1473, 84 MAR 83 APR edition may be used until exhausted.
All other editions are obsolete.

SECURITY CLASSIFICATION OF THIS PAGE
UNCLASSIFIED

TABLE OF CONTENTS

I. INTRODUCTION

Adiabatic shear banding is the name given to a localization phenomenon that occurs during rapid plastic deformation of many materials, including both metals and plastics. The process is usually thought of as coming about in the following manner. Plastic deformation heats the material locally, and if the flow stress decreases with increasing temperature, there is the possibility that thermal softening will overcome strain and strain-rate hardening and that stress will subsequently decrease with further straining. When net softening occurs, the material becomes extremely sensitive to inhomogeneities, and the deformation tends to accumulate in narrow regions where the plastic strain-rate is enormous, whereas in neighboring regions the material may even return to a purely elastic state. As localization occurs and the deformation becomes extremely inhomogeneous, heat conduction tends to damp the process.

Shear banding of this type is a major damage mechanism that can occur in machining and forming processes as well as during impact and penetration. Bands may form as macroscopic failure surfaces or as distributed microscopic damage. Many examples of naturally occurring shear bands are given in references 1-4, and in references 5-7 controlled shear experiments, designed specifically to produce isolated shear bands, are reported. Photomicrographs in those articles give a good idea of the morphology and scale of individual bands, which vary in thickness from less than 1 micron to more than 100 or 150 microns, with lateral extent in the plane of the band being many, many times its thickness. In general it appears that when shear bands form, they cut through the underlying metallurgical structures indiscriminately so that a continuum model, based on gross physical properties, can be expected to give an accurate description.

In references 5-7 the experimental data is resolved either in space or in time, but not in both simultaneously. Data exhibiting both space and time resolution during the formation and development of a single band would be of considerable importance for further theoretical advances.

II. CONTINUUM FORMULATION

According to the general description given above, a proper continuum setting for the phenomenon should treat finite deformations of a thermo-visco-plastic material, and therein lie several substantial problems. Namely, there is no generally agreed upon version of plasticity for finite deformations in existence today; the same is true for viscoplasticity even for small deformations; and heat conduction and heat generation from plastic dissipation only make the situation more unsatisfactory. In this report, as in all the other recent literature on adiabatic shear banding, these problems are largely bypassed or ignored by restricting consideration to a one-dimensional initial-boundary value problem for a very highly idealized material. The way in which a theoretical description of shear band formation should be embedded in a three-dimensional theory, with proper account being taken of finite deformations, invariance requirements, finite band size in lateral direction, etc., remains as a major problem for the future.

Accordingly, consider a block of incompressible material with upper and lower boundaries at $\bar{Y} = \pm H$ and undergoing only a simple shearing motion in the $\bar{X}$ direction

$$\bar{x} = \bar{X} + \bar{u}(\bar{Y},\bar{t}) \ , \ \bar{y} = \bar{Y}, \ \bar{z} = \bar{Z}, \tag{1}$$

and all dependent variables depend only on the space coordinate $\bar{Y}$ and time $\bar{t}$. The overbar signifies a dimensional quantity. Since shear bands are observed to be extremely thin with respect to their lateral extent, this motion is intended to simulate the actual motion far from the edges of the band. In nondimensional terms the governing equations may be written as follows.

Momentum: $$\rho v_{,t} = s_{,y} \tag{2}$$

Energy: $$\theta_{,t} = k\theta_{,YY} + s\dot{\gamma}_p \tag{3}$$

Constitutive: $$s_{,t} = \mu(v_{,Y} - \dot{\gamma}_p) \tag{4}$$

$$\kappa_{,t} = \frac{sh(\kappa)}{\kappa}\,\dot{\gamma}_p \tag{5}$$

Yield: $$f(s,\theta,\dot{\gamma}_p) = \kappa \tag{6}$$

Boundary conditions are taken to be

$$v(\pm 1,t) = \pm 1, \ \theta_{,Y}(\pm 1,t) = 0 \tag{7}$$

and only solutions with θ and $v_{,Y}$ symmetric about $y = 0$ are considered. In these equations $v = u_{,t}$ is particle velocity, s is shear stress, θ is temperature change, κ is a work hardening parameter, and $\dot{\gamma}_p$ is the plastic strain rate. These variables are related to the dimensional (barred) quantities as follows.

$$\begin{aligned} &Y = \bar{Y}/H, \ t = \dot{\gamma}_0\bar{t}, \ v = \bar{v}/H\dot{\gamma}_0, \ \dot{\gamma}_p = \dot{\bar{\gamma}}_p/\dot{\gamma}_0 \\ &s = \bar{s}/\kappa_0, \ \kappa = \bar{\kappa}/\kappa_0, \ \theta = \bar{\rho}c\bar{\theta}/\kappa_0 \end{aligned} \tag{8}$$

In addition nondimensional constants have been introduced for density, thermal conductivity, and elastic modulus. Respectively these are

$$\rho = \bar{\rho}H^2\dot{\gamma}_0{}^2/\kappa_0, \ k = \bar{k}/\bar{\rho}cH^2\dot{\gamma}_0, \ \mu = \bar{\mu}/\kappa_0 \tag{9}$$

In (7) and (8) $\dot{\gamma}_0 = \bar{v}(H,\bar{t})/H$ is the characteristic strain rate, κ_0 is the initial yield stress, and c is the specific heat of the material.

In writing down equations (2)-(6), a number of implicit simplifying assumptions have been made. In (3) it has been assumed that the elastic and thermal parts of the internal energy are completely decoupled so that there is no thermoelastic effect. In particular there is no thermal expansion, c does not depend on strain, and the elastic modulus does not depend on temperature. The term $s\dot{\gamma}_p$ in (3) is the rate of plastic work, and it is assumed to be

converted completely into heat. In (4) it has been assumed that the total strain rate may be decomposed into the sum of elastic and plastic parts, and that the stress is a linear function of elastic strain. In equation (5) the function $h(\kappa)$ is the slope of a reference isothermal stress strain curve. The equation assumes that the work hardening parameter, κ, evolves according to the plastic work done, so that its evolution is the same in a slow isothermal test as in a rapid adiabatic test. Equation (6) states that the yield surface depends on the plastic strain rate, as well as stress and temperature. If $\dot{\gamma}_p = 0$, then the equation simply gives the static yield surface in stress temperature space. It is natural to assume that the function f has the properties $f_s > 0$, $f_\theta > 0$, and $f_{\dot{\gamma}_p} < 0$. Thus if $f(s,\theta,0)$ is greater than κ, plastic flow occurs, and if it is less than or equal to κ, the plastic strain rate is zero, and the material deforms only elastically.

Alternatively, by inverting (6) it is possible to write a rate equation for $\dot{\gamma}_p$.

$$\dot{\gamma}_p = g(s,\theta,\kappa) \tag{10}$$

where to be consistent the function g must have the properties $g_s > 0$, $g_\theta > 0$, and $g_\kappa < 0$. In this form it is clear that κ and γ_p have the status of internal variables, which are controlled by rate equations.

In the preceding discussion it has been assumed that there is a definite yield surface where the plastic strain rate vanishes. Many authors prefer to use (10), but without a definite yield surface, for ease in computations. Several examples of this approach are to be found in reference 21, but in every case it turns out that there is a transition region where the plastic strain rate becomes extremely small and the deformation is essentially elastic.

In all the calculations described in this paper, the functions g and h have been taken as follows.

$$g(s,\theta,\kappa) = \frac{\operatorname{sgn} s}{b}\left\{\left[\frac{|s|}{\kappa(1-a\theta)}\right]^{1/m} - 1\right\}, \quad h(\kappa) = \frac{n}{\psi_o}\,\kappa^{\frac{n-1}{n}} \tag{11}$$

These are empirical functions, which are intended to be fit to representative data for particular materials. They will be more readily recognized in the forms

$$|s| = \kappa(1-a\theta)\,(1+b|\gamma_p|)^m, \qquad \kappa = \left(1+\frac{\psi}{\psi_o}\right)^n$$

where ψ is plastic strain in a reference test. Equation (11) has introduced five more nondimensional constants, namely

$$n,\ \psi_0,\ b = \bar{b}\dot{\gamma}_0,\ m,\ a = \frac{\bar{a}\kappa_o}{\bar{\rho}c} \tag{12}$$

The first one is known as the work hardening exponent, the second can be used to adjust the slope at first yield for the reference curve, $\bar{b}$ is a characteristic time, m is the rate hardening exponent, and $\bar{a} = d\bar{s}/d\bar{\theta}$ is the

slope of the thermal softening curve, which has been assumed to be linear. In equations (9) and (12) there are eight independent nondimensional parameters in all that control the behavior of the response. Of the eight, only three contain the externally imposed quantities H and $\dot{\gamma}_0$, and five are determined entirely by intrinsic physical properties of the material. In any case it is to be expected that the overall response may be quite different in different regions of parameter space, and because there are so many independent parameters, it may be some time before the full range of effects can be known.

III. RESULTS OF FINITE ELEMENT CALCULATIONS

In two other papers[16,17] the results of finite element calculations for the system of equations (2)-(5) and (11) have been described in some detail. Some of the principal features of those calculations are summarized here.

First note that the equations have solutions with v = Y and all other response functions independent of Y. Examples of these so-called homogeneous solutions for particular choices of the eight parameters have been given in reference 17 and are shown in Figure 1. The choice a = b = 0 generates the reference stress strain curve, and the choice a = 0 generates an isothermal response curve for each applied strain rate. When both a and b have finite values, the response curve starts out like an isothermal curve, but as the plastic work accumulates, the temperature rises and softening begins. Finally at a critical strain the stress response reaches a maximum, denoted P in the figure, and decreases thereafter. This type of behavior for thermal softening materials is well known (eg., references 5,7,8,11-14 and others), although the details of the thermo-visco-plasticity models vary among the various authors. In fact the softening response is typical for many cases of materials with damage, with the damage often being represented by internal variables. Softening may also be induced by geometric changes, the most familiar example being change of cross sectional area in a tension test.

No matter what its origin, once softening begins there is opportunity for localization to occur. With the system of equations described above the onset of localization has been observed by adding a temperature perturbation to the homogeneous solution and restarting the finite element calculation as a new initial-boundary value problem. The perturbation was positive and symmetric about the center of the interval, and it was added at the point marked I in Figure 1, just before the peak homogeneous stress. Complete details have been given in reference 16.

Two cases were considered: one with central height of the temperature bump $\Delta\theta = 0.1$ and width 0.5, and one with 1/5th the height and width of the first. The stress response which is nearly constant in Y, is shown in Figure 2. In the case of the smaller perturbation the stress follows the homogeneous response rather closely at first, until well past the peak homogeneous stress, but eventually the response deviates abruptly, and the stress appears to collapse. For the larger perturbation the pattern is similar except that stress collapse sets in even before peak homogeneous stress. In both cases cross sectional plots of temperature or plastic strain rate at fixed times show large peaks developing in the center of the interval as the stress collapses. At the end of the calculation the central value for $\dot{\gamma}_p = \bar{\dot{\gamma}}_p/\dot{\gamma}_0 > 60$. As

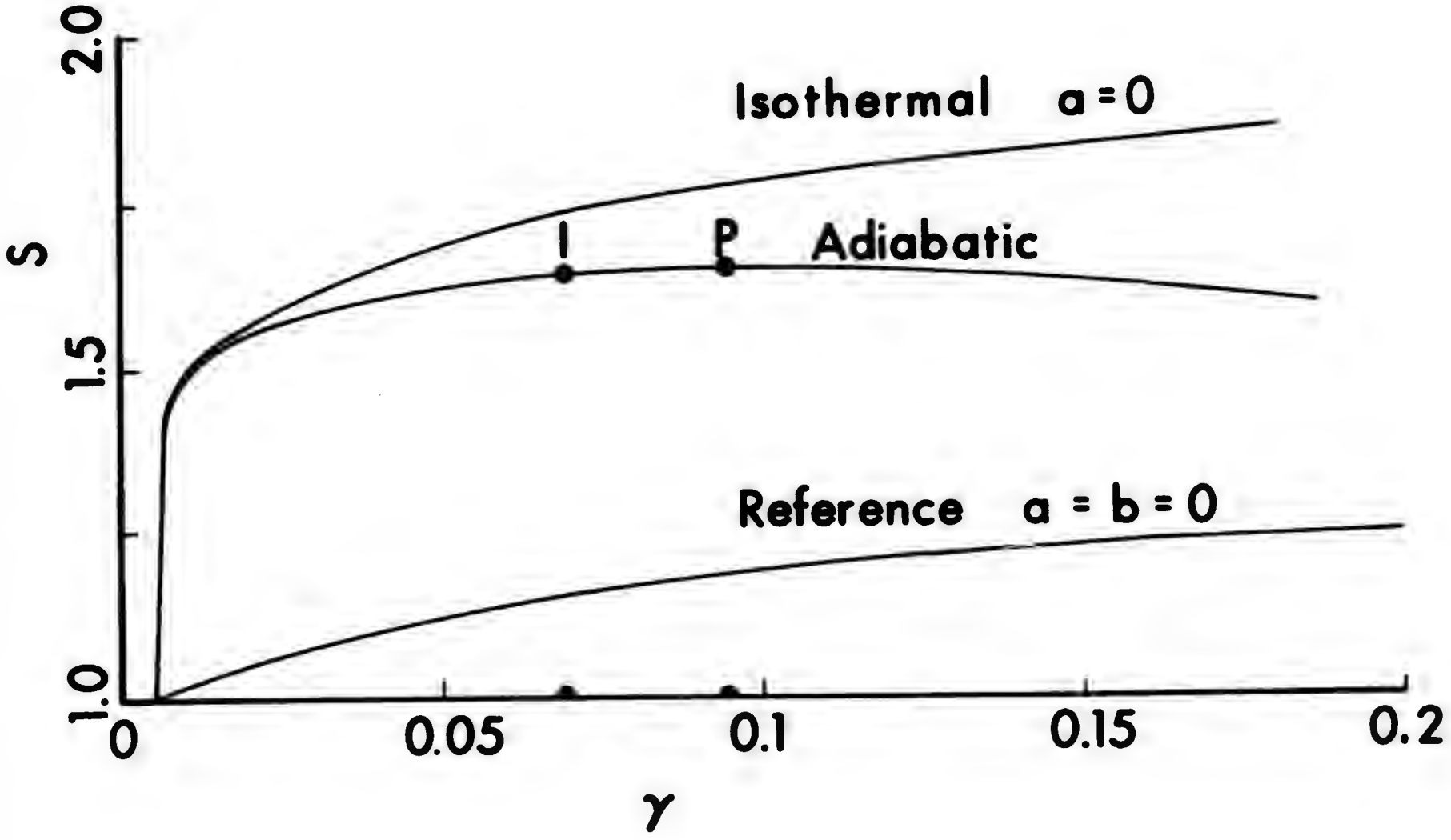

Figure 1. Sketch of Typical Reference, Isothermal and Adiabatic Stress Strain Response for Homogeneous Deformation

the central peaks develop, the plastic strain rate drops to zero at the edges of the interval, and the temperature becomes constant there since plastic working vanishes with plastic strain rate. Calculations for finite deformations have also been reported in references 7 and 13-15 where somewhat different versions of visco-plasticity or just nonlinear elasticity were used. Delayed stress collapse was noted in reference 13, as well, so that the phenomenon appears to be generic for softening behavior and not specific for the particular constitutive description used.

IV. ESTIMATE FOR THE MAXIMUM CRITICAL TIME OF STRESS COLLAPSE

Figure 2 is reminiscent of curves for imperfection sensitivity in a bifurcation problem. All that is missing is the bifurcation branch itself. In the usual buckling problem some measure of deflection is plotted against an external loading parameter. As the load increases, no change occurs in the perfect system until a critical load occurs where the possible solution paths in load-deflection space split into multiple branches. These principal bifurcation branches represent limiting behavior for an imperfect system so they give useful information about the response, although the imperfection sensitivity may be such that, as a practical matter, it is extremely difficult to approach the ideal response. From this point of view there should be a curve (or curves) in Figure 2 that breaks off from the homogeneous response, plunging steeply and lying somewhat to the right of both perturbation curves. such a curve would indicate the largest strain that could ordinarily be achieved without localization. References 22-24 discuss bifurcation and stability in the context of elastic, plastic, and general systems (mostly in steady motion) respectively.

In the present case time plays the role of the external load, but it is much more than just a passive parameter, as in a static buckling problem, since here it is also an independent variable in the differential equations. In an attempt to examine the stability of the homogeneous response, several authors have considered the equations of first variation with respect to the homogeneous response (references 8-12 and 14), and that will be the approach taken here. With the variations expressed as $v = \tilde{v} - v_H$, etc., where the subscript indicates the homogeneous response, the linearized variational equations have the form

$$u_{,t} = Lu + A(t)u \tag{13}$$

where $u = (\tilde{v},\tilde{s},\tilde{\theta},\tilde{\kappa})$, L is a linear matrix differential operator that contains first and second derivatives on Y, and A(t) is a time dependent matrix with entries determined by the homogeneous motion. Homogeneous boundary conditions for (13) are $\tilde{v}(\pm 1,t) = \tilde{\theta}_{,Y}(\pm 1,t) = 0$.

In previous work the variational equations have usually been treated either as an initial-boundary value problem or as a system with constant coefficients. Since the coefficients are not constant, the latter approach tacitly assumes without further justification that in some sense the coefficients are slowly varying in comparison with the solutions to be found. When treated as an initial-boundary value problem, it is always found that

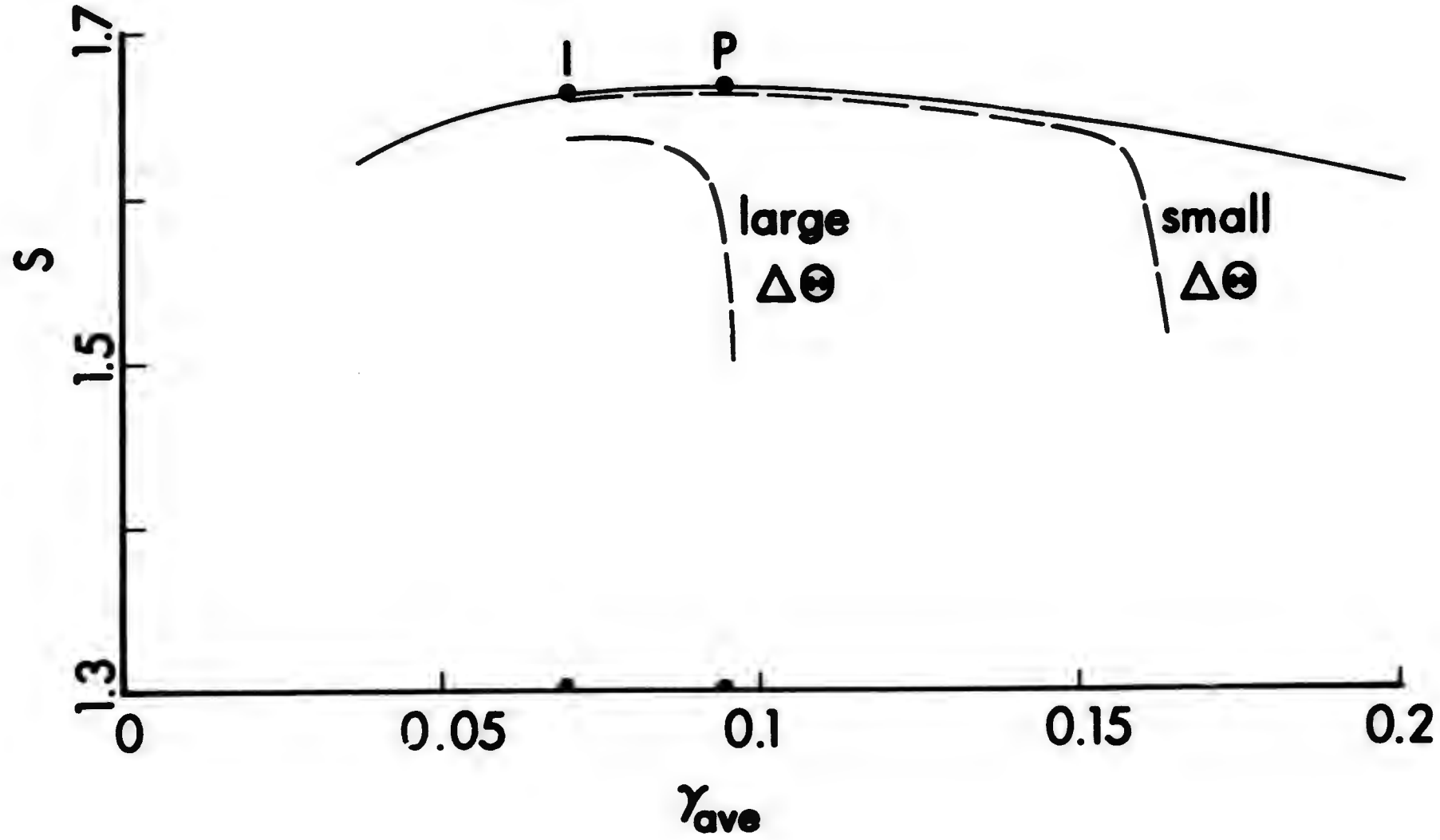

Figure 2. Response to Temperature Perturbations

solutions can begin to grow exponentially once the peak in the homogeneous response has been passed. However, it is also always found that the rate of growth is far too small to explain the most important aspects of observed behavior. In fact the growth of the perturbation in Figure 2 for the smaller disturbance is approximately exponential at first, but at a very low rate, and the early behavior gives no hint about the timing for stress collapse. In view of the results shown in Figure 2 it seems likely that the treatment as an initial-boundary value problem can only give limited information about the sensitivity to infinitesimal imperfections, and no information at all about either the point of bifurcation or the bifurcation branch. In reference 11 the use of a Liapunov function provides a third approach to examine stability and is used to analyze the unsteady shearing of a thermoviscous fluid, that is, a Newtonian fluid with a temperature dependent viscosity. However, a complete bifurcation analysis is not actually carried through, the difficulty being that solutions of the perturbation equations with the time dependent coefficients are not known.

When the left hand side of (13) is multiplied through by the row matrix $(\tilde{v},\tilde{s},\beta\tilde{\theta},\alpha\tilde{\kappa})$, where β and α are arbitrary (at this stage) but positive weights, it becomes the exact derivative of a sum of squares. After integration over the interval followed by use of the boundary conditions and division of both sides by the integral of the weighted sum of squares, (13) becomes

$$\frac{1}{E}\frac{dE}{dt} = \frac{1}{E}\left\{ - \beta k \int_I \tilde{\theta}_{,Y}^2 \, dY + A_{ij}^s(t) \int_I u_i u_j dY \right\}$$

$$= \Lambda\,(\tilde{v},\beta\tilde{\theta},\tilde{\kappa}) \qquad \text{i.e., } \Lambda = \Lambda(....) \tag{14}$$

$$\text{where } E = \frac{1}{2}\int_I (\rho\tilde{v}^2 + \frac{1}{\mu}\tilde{s}^2 + \alpha\tilde{\kappa}^2 + \beta\tilde{\theta}^2)\, dY$$

For all possible solutions of (13) we would like to know when the right hand side of (14) can first become positive. Thus for each value of time it is necessary to look for the maximum over solutions of (13). Only the symmetric part of A_{ij} enters into (14), and the most advantageous choices for α and β will be left for later.

Rather than maximizing over solutions, which are unknown, it is easier to regard the right hand side as a Rayleigh quotient for which stationary values are sought among all smooth functions which satisfy the boundary conditions. Since this set of functions contains the solutions, the maximum for the Rayleigh problem will be an upper bound for the original problem, and the time when the Rayleigh quotient first turns positive will be a lower bound for the critical time in the original problem. This approach for estimating the bifurcation point when the coefficients are time varying was introduced by Serrin[25] and has been used to advantage in unsteady fluids problems by Neitzel and Davis[26]. The addition of the free constants in the present case should allow some optimization of the estimate.

To illustrate this idea consider the simple case where $\kappa = 1$ and $\mu = \infty$. Then the homogeneous problem has the solution

$$v_H = Y,\ \dot{\gamma}_{pH} = 1,\ s_H = (1 + b\,\dot{\gamma}_{pH})^m\,(1 - a\theta_H)$$

$$(1 - a\theta_H) = \exp\left\{-a(1 + b)^m t\right\} \tag{15}$$

and the Rayleigh problem becomes

$$\Lambda = \frac{1}{E}\left\{-\beta k \int_I \tilde{\theta}^2{}_{,y}\, dY + A^s_{\alpha\beta}(t) \int_I u_\alpha u_\beta dY\right\} \tag{16}$$

where now $E = \frac{1}{2}\int_I (\rho\,\tilde{v}^2 + \beta\tilde{\theta}^2)\, dY$, $u = (\tilde{s},\tilde{\theta})$ and the matrix A is given by

$$\{A\} = \begin{Bmatrix} -g_s & -g_\theta \\ \beta(sg)_s & \beta(sg)_\theta \end{Bmatrix} \tag{17}$$

The plastic strain rate, $\dot{\gamma}_{pH} = g(s_H,\theta_H)$ is found by inverting $(15)_3$. Next $\tilde{s}$ is eliminated in favor of $\tilde{v}$ and $\tilde{\theta}$ by using the exact perturbation equation

$$s = -\frac{1}{A_{11}}(\tilde{v}_{,Y} + A_{12}\,\tilde{\theta}) \tag{18}$$

Now the Rayleigh quotient, considered as a variational problem, leads to two coupled, second order, ordinary differential equations in $\tilde{v}$ and $\tilde{\theta}$ with Λ as an eigenvalue. The choice

$$\tilde{v} = \tilde{v}_o \sin \lambda_j Y,\ \tilde{\theta} = \tilde{\theta}_c \cos \lambda_j Y$$

$$\lambda_j = j\pi,\ j = 1,2,3....$$

has the desired symmetry about $Y = 0$ and satisfies the necessary boundary conditions. the characteristic matrix is symmetric so the eigenvalues are real, and the characteristic equation for Λ turns out to be

$$\Lambda^2 - \left\{-2k\lambda_j^2 - \frac{2\lambda_j^2}{\rho g_s} - \frac{2g\,g_\theta}{g_s}\right\}\Lambda + \left\{\frac{4k\lambda_j^2}{\rho g_s} - \frac{[\beta(sg)_s - g_\theta]^2}{\beta\rho g_s{}^2} - \frac{4sg_\theta}{g_s}\right\}\lambda_j^2 = 0 \tag{19}$$

From the sign of the coefficients (19) it is clear that

$$\Lambda^{(1)} + \Lambda^{(2)} < 0, \text{ always}$$

and

$$\Lambda^{(1)}\,\Lambda^{(2)} > 0, \text{ provided that} \tag{20}$$

$$[(-1 + m)x - a]^2 - 4k\lambda^2{}_j\, m(1 + b)^{-m}\, x < 0 \tag{21}$$

where $x = \beta(1 - a\theta)$. When (20) and (21) hold, both eigenvalues are negative, and therefore, the left side of (16) is guaranteed to be negative for all solutions of the perturbation equations. The left hand side of (21) is a parabola in x that opens upwards and has two real positive roots, $r_1 > r_2 > 0$. The constant β has not yet been chosen, but since x decreases with increasing t, and since $\theta(0) = 0$, the best choice is $\beta = r_1$. Then the left hand side of (21) will be less than or equal to zero from $t = 0$ until the time when $x = r_2$. That is to say, for the perturbation problem

$$\frac{1}{E}\frac{dE}{dt} \leq 0 \quad \text{if } t \leq \frac{1}{a(1+b)^m} \ln \frac{r_1}{r_2} \tag{22}$$

and equality in $(22)_2$ gives a lower bound estimate for the critical bifurcation time. Note that since the two roots r_1 and r_2 depend on the bifurcation mode j, there is actually a sequence of increasing, critical bifurcation times that corresponds to increasing mode numbers $j = 1,2,3...$

It turns out that if either the (nondimensional) thermal conductivity or the rate sensitivity m vanishes, then $r_1 = r_2$ for all modes so the best estimates for the critical bifurcation times are all $t = 0$. As one final comment, note that having an estimate for the critical bifurcation time only provides an estimate for the time of stress collapse in the case of infinitesimal perturbations; it does not provide an estimate for any case of finite perturbation.

The success of this approach for the simple example given above shows that it holds promise for the more general case, which will be reported in a future report.

V. STEADY SOLUTIONS

Equations (2)-(6) also have steady solutions, where the four variables (v,s,κ,θ) depend only on the spatial coordinate Y, but not on time t. For this to be strictly true, equation (5) implies that $h(\kappa) = 0$ throughout the whole interval, which in turn implies that κ is constant. That is to say, the material has saturated with respect to work hardening. Since $s = \text{const}$ by (2), and (6) can be solved to get $\dot{\gamma}_p = \Gamma(\theta;s,\kappa)$, equation (3) reduces to an ordinary differential equation in θ with a first integral

$$\frac{1}{2}\theta,_Y^2 = \frac{s}{\kappa}\int_{\theta}^{\theta_c} \Gamma \, d\theta \tag{23}$$

where θ_c is the temperature at the center of the band. Equation (23) may be solved by quadrature to obtain a solution of the form

$$Y = F(\theta;\theta_c,s,\kappa) \tag{24}$$

Since the saturation flow stress κ may be regarded as a material property, equation (24) shows that in general there is a two parameter family of steady solutions for a given material. Once (23) has been obtained, the velocity field may be found by integrating the steady version of (4). Typical profiles are shown in Figure 3. To give a better idea of the physical scaling in a shear band, for the Litonski law in (11) equation (24) may be written as

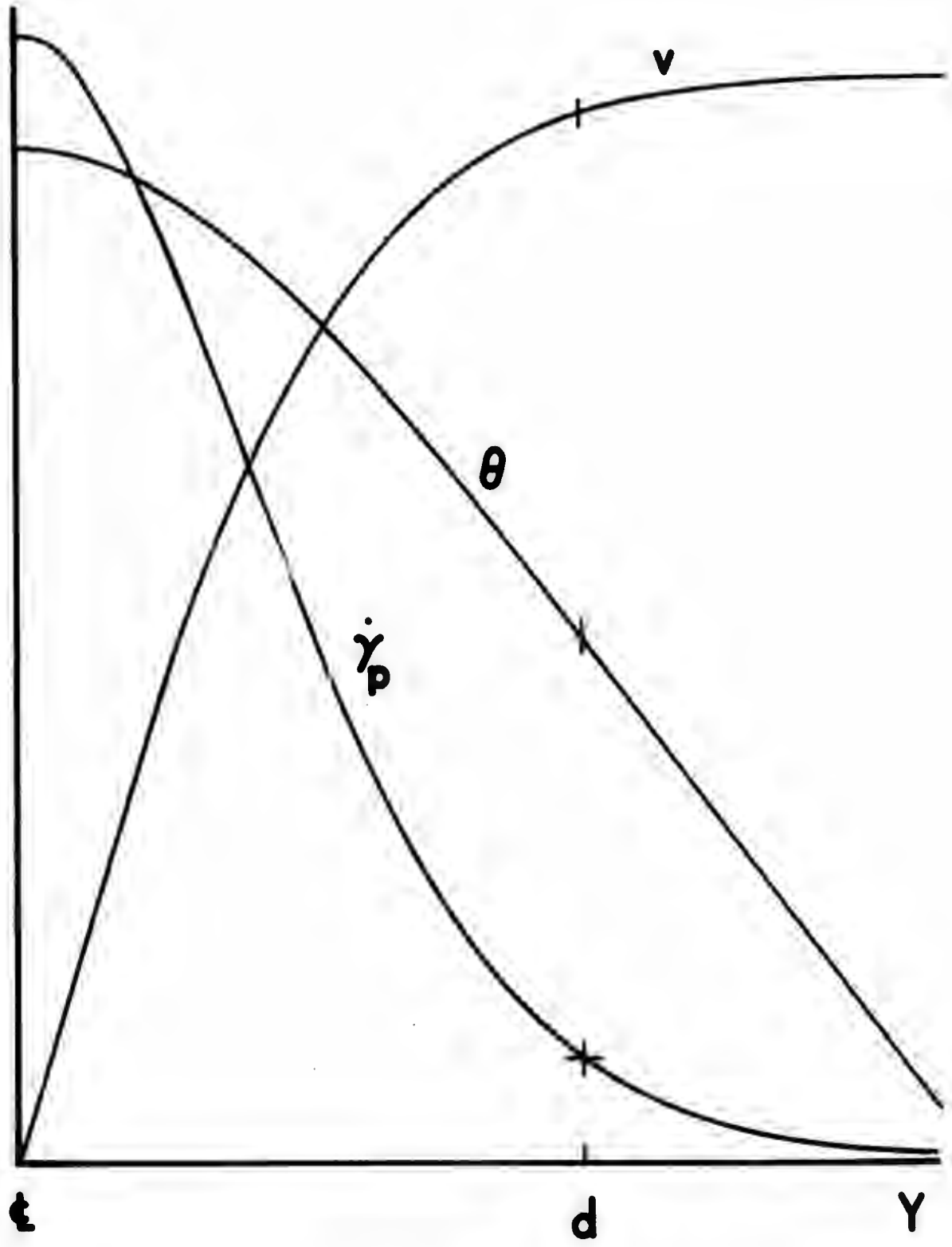

Figure 3. Typical Configuration for Steady Response

$$\bar{Y} = \frac{1}{\sqrt{2}}\sqrt{\frac{\bar{b}\bar{k}}{\bar{a}\bar{\kappa}}}\left(\frac{1-\bar{a}\bar{\theta}_c}{1-\bar{a}\bar{\theta}_a}\right)^{\frac{1+m}{2m}}\int_0^{\frac{\bar{a}(\bar{\theta}_c-\bar{\theta})}{1-\bar{a}\bar{\theta}_c}} \frac{dt}{t^{\frac{1}{2}}\left\{\frac{m}{1-m}\left[\frac{1-\left(\frac{1}{1+t}\right)^{\frac{1-m}{m}}}{t}\right]-\left(\frac{1-\bar{a}\bar{\theta}_c}{1-\bar{a}\bar{\theta}_a}\right)^{\frac{1}{m}}\right\}^{\frac{1}{2}}} \qquad (25)$$

where $\bar{Y} = 0$ locates the center of the band. In this form all quantities are dimensional, and the residual integral is O(1). $\bar{\theta}_a$ is the temperature where $\dot{\bar{\gamma}}_p = 0$, and there $\bar{s} = \bar{\kappa}(1 - \bar{a}\bar{\theta}_a)$ holds. Note the square root scaling on the basic physical quantities, but note especially the extremely strong dependence on the temperature contrast between the center and the edge of the band when the strain rate sensitivity is small. Typical values for m in many metals are around 0.02. The temperature term may also be written

$$\frac{1-\bar{a}\bar{\theta}_c}{1-\bar{a}\bar{\theta}_a} = (1+\bar{b}\dot{\bar{\gamma}}_p^c)^{-m}$$

so for m small and $\bar{b}\dot{\bar{\gamma}}_p^c$ large (the usual case) the length scale varies nearly as the inverse square root of the central plastic strain rate and only weakly with $\bar{b}$.

In Figure 3, d is defined arbitrarily as the distance from the center of the band where the plastic strain rate has fallen to 1/10th its central value. At that distance the velocity has nearly reached its extreme value and the temperature gradient has become nearly constant. Thus, it gives a convenient point for measuring the size and strength of the shear band. The following table shows typical results for a realistic material.

Table 1. Shear Band Values for $\bar{\theta}_c = 400^{\circ}K$ and Various Strain Rates

$\dot{\bar{\gamma}}_p^c$, s^{-1}	d, μm	$\bar{\theta}(d)$, $^{\circ}K$	$\bar{v}$, m/s	$\bar{s}$, GPa
10^3	138	334	0.076	0.467
10^4	43	334	0.234	0.489
5×10^4	19	334	0.514	0.505

Note that the temperature difference in the band is not large, but the plastic strain rate varies by a factor of 10 over distances measured in 10's or at most 100's of microns. These characteristic values have been computed using realistic numbers for the material constants of a strong steel, so it is encouraging that the numbers come out in the right general range for known experimental values.

The steady solutions by themselves are of limited utility because they tend to constant, and rather large, temperature gradients away from the center, as can be seen by rough estimation from values in the table. However, note that when the time in (2)-(5) is scaled according to the rule $t = \tau/\delta$, where δ is a small parameter, then the steady equations (vanishing left hand sides) result in the limit as $\delta \to 0$. With τ being held fixed, $t \to \infty$, so the

steady equations apparently have the interpretation of holding asymptotically at large times. But since they cannot meet arbitrary boundary conditions away from the center, they must hold only in a central boundary layer. With that interpretation the outer configuration of the steady solutions defines inner boundary values for an exterior solution. The steady solutions and their probable interpretation as boundary layers will be explored in a future report.

VI. THE ESSENTIAL EMBEDDED PROBLEM

Another point of view has been suggested by Varley[27], namely that the essential features of the localization type of material response can be captured by some simpler problem, which is embedded within the full set of equations. From that point of view many of the mathematical complications stem from "small higher order terms" that modulate the basic response. To look for a simpler embedded problem, consider the special case of a rigid/plastic, non heat conducting, and non rate sensitive material. With $\mu = \infty$, and $k = f_{\dot{\gamma}_p} = 0$, equations (2)-(6) become

$$s_{,y} = v_{,t}, \qquad v_{,y} = p$$
$$\kappa_{,t} = \frac{s}{\kappa} h(\kappa)p, \quad \theta_{,t} = sp \tag{26}$$
$$s = \kappa g(\theta)$$

where $p = \dot{\gamma}_p \geq 0$ and $g(\theta)$ carries the temperature sensitivity of the material. When $p = 0$, unloading occurs, and in an unloaded region the stress is constant. With v eliminated from the first two equations and sp eliminated from the next two, (26) becomes

$$s_{,YY} = \rho p_{,t}, \quad M(\kappa) = \theta + A(Y), \quad s = S(\theta) \tag{27}$$

In (27) $M(\kappa)$ is a monotonically increasing function since $h(\kappa)$ is positive, $A(Y)$ is an arbitrary function, and in $S(\theta)$ the dependence on Y has been suppressed. Since $g(\theta)$ must be a decreasing function to represent thermal softening, it is not difficult to find combinations of $g(\theta)$ and $h(\kappa)$ such that the function $S(\theta)$ has a single maximum. For example for linear work hardening with constant modulus G_p and and linear thermal softening, the stress is given by $s = S(\theta) = \sqrt{2G_p(\theta+A)}\ (1-a\theta)$, which has a maximum at $\theta_m = \frac{1}{3a}[1-2aA(Y)]$.

It may be assumed that θ_m is positive as shown in Figure 4a. Now with the aid of $(26)_4$ and $(27)_3$ the momentum equation (27) becomes

$$[S(\theta)]_{,YY} = \rho \left[\frac{\theta_{,t}}{S(\theta)}\right]_{,t} \tag{28}$$

This equation is hyperbolic when $S_\theta > 0$ and elliptic when $S_\theta < 0$, and since θ can only increase, each point either evolves toward the hyperbolic/elliptic transition and beyond or else unloading occurs. Figure 4b shows a sketch of the conjectured domains for a typical initial/boundary value problem. Alternatively the H-E boundary would extend to $Y = \pm 1$, and the E-U boundary would come in from the sides at a later time. In either case both θ and $\theta_{,t}$

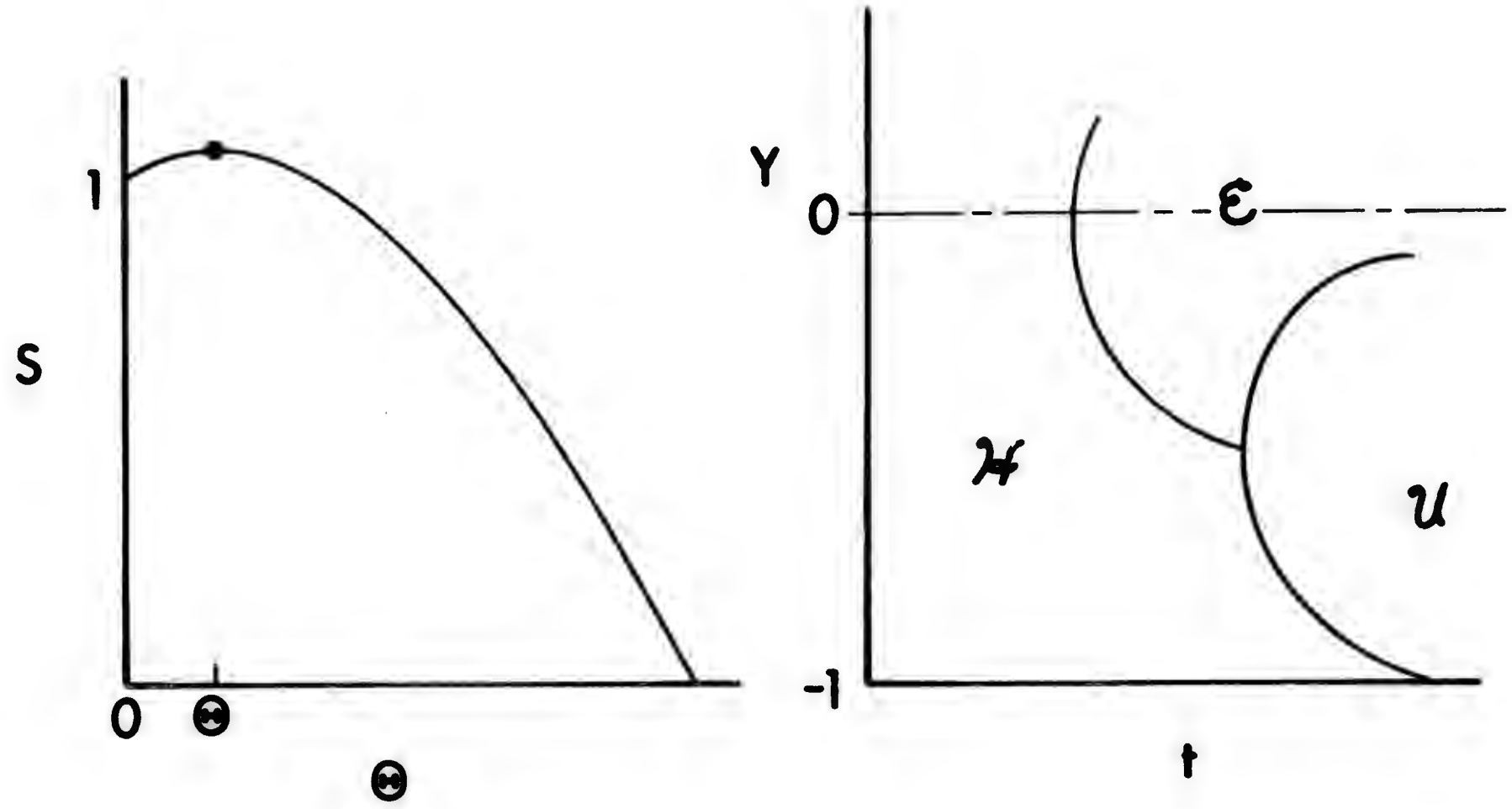

Figure 4. a. Sketch of Stress-Temperature Response in the Absence of Heat Conduction and Viscous Effects for A rigid-Plastic Material. b. Conjectured Hyperbolic, Elliptic, and Unloaded Regions for an Initially Inhomogeneous Temperature Distribution

would be specified along part of the boundary of the E-region, which will generally tend to produce singular behavior at later times in accordance with Varley's conjecture. Without heat conduction or a rate effect there is no mechanism to limit the singularity.

VII. DIPOLAR PLASTICITY

Since large temperature and strain gradients occur during localization, it seems reasonable to examine the consequences of using a dipolar type theory of plasticity, as formulated by Green, McInnis, and Naghdi[28]. A rate sensitive version of the dipolar theory has been set down by Wright and Batra[17]. The equations have homogeneous solutions, which are the same as for the simple case, and preliminary perturbation calculations of the same type as discussed above indicate that the dipolar effect is stabilizing as the homogeneous response changes from increasing stress to decreasing stress, much in the same way that bending stiffness in a thin wire is stabilizing as the axial force changes from tension to compression. Further calculations are in progress.

VIII. CONCLUSIONS

In order to develop adequate damage models for use in ballistic impact calculations, it is desirable to obtain as much information as possible from direct examination of the proposed damage mechanism. This approach, which may be called micromechanics, holds out the promise of providing a rational basis for the damage model that relies to the maximum extent possible on standard laboratory mechanical tests and handbook data, and minimizes extensive, special purpose characterization.

In this report an attempt has been made to summarize the current understanding of one major damage mechanism, namely adiabatic shear bands, and to outline some numerical and analytical work, either in progress or else proposed as likely to deepen understanding. The greatest amount of work so far has been in terms of a one dimensional formulation, but as was pointed out there remain many serious questions regarding the proper way to embed the theory in a three dimensional context. In any case the proper setting is viscoplasticity for a work hardening and thermal softening material with heat conduction.

To date theoretical perturbation studies have indicated that material response becomes unstable and susceptible to localization once the stress response curve for homogeneous deformation achieves a maximum. However, the predicted rate of growth of the localization always turns out to be too small to match experimental evidence. Nonlinear calculations have shown that although the temperature and plastic strain rate do begin to localize at the point predicted by linear perturbation analyses, the stress does not deviate markedly from the homogeneous response until a strain has been reached that may lie well beyond the predicted point. A first attempt at a bifurcation analysis that uses a Liapunov function seems to confirm this result.

Calculations and analyses of the kinds described above are directed toward the initiation stages of shear band formation, but have no bearing on late stage developments or residual strength capacity. Steady solutions of the governing equations, which do exist under certain conditions and whose solutions can be written down as quadratures, seem to be related only to the late stage developments. In fact sample calculations give characteristic geometries which appear to have the correct order of magnitudes for comparison with experiments, and strongly suggest that a steady solution corresponds to a boundary layer within the core of a shear band.

From the analytical point of view the full nonlinear problem is parabolic because of rate effects and heat conduction. These two physical effects are controlled by small parameters; however, and in the limit of these parameters vanishing, the equations show a change of type from hyperbolic to elliptic when the stress response reaches a maximum. Thus another promising way to view the full set of equations is that they contain an embedded change of type, which is the real driver of the localization, and that the higher order effects of heat conduction and viscosity modulate the intensity of localization. It is intended to explore this point of view, which may be expected to lead to a completely new kind of perturbation analysis.

One final variation of the governing equations introduces a gradient sensitivity into the problem because extremely large strain and temperature gradients seem likely to occur during formation of a shear band. Preliminary calculations indicate that a gradient effect tends to stiffen the material and to retard the formation of bands.

A brief bibliography at the end of this report will serve to introduce the interested reader to most aspects of adiabatic shear bands, but the field is an active one and the literature is growing rapidly, so the list is by no means complete.

REFERENCES

Material Aspects, Occurrence, and Qualitative Description

1. Rogers, H.C., Adiabatic Shearing - General Nature and Material Aspects in Material Behavior Under High Stress and Ultrahigh Loading Rates Sagamore Army Materials Research Conference Proceedings 29, eds. J. Mescall and V. Weiss, Plenum Press, New York (1983) 101-118 (see also Rogers, An. Rev. Mat. Sci. 9 (1979) 283).

2. Semiatin, S.L., Lahoti, G.D., and Oh, S.I., The Ocurrence of Shear Bands in Metalworking, Sagamore 29, 119-160.

3. Hutchings, I.M., The Behavior of Metals Under Ballistic Impact at Sub-Ordnance Velocities, Sagamore 29, 161-198.

4. Grady, D.E., Asay, J.R., Rohde, R.W., and Wide, J.L., Microstructure and Mechanical Properties of Precipitation Hardened Aluminum Under High Rate Deformation, Sagamore 29, 81-100.

Experimental Observations on Isolated Bands

5. Costin, L.S., Crisman, E.E., Hawley, R.H., and Duffy, J., On the Localization of Plastic Flow in Mild Steel Tubes Under Dynamic Torsional Loading, in Mechanical Properties at High Rates of Strain, Proc. 2nd Oxford Conf. 1979, ed. J. Harding, Inst. Phys., London (1980) 90-100.

6. Moss, G.L., Shear Strains, Strain Rates, and Temperature Changes in Adiabatic Shear Bands, in Shock Waves and High-Strain-Rate Phenomena in Metals, ed. M.A. Meyers and L.E. Murr, Plenum Press, New York (1981) 299-312 (see also Technical Report ARBRL-TR-02242 Ballistic Research Laboratory, Aberdeen Proving Ground, MD 21005, May 1980).

7. Lindholm, U.S. and Johnson, G.R., Strain-Rate Effects in Metals at Large Shear Strains, Sagamore 29, 61-79 (see also Johnson, Hoegfeldt, and Lindholm, J. Eng. Mat. and Tech., Trans. ASME 105 (1983) 42-47 and 48-53).

Linear Stability Analyses

8. Clifton, R.J., Adiabatic Shear Banding, Chap. 8 in Materials Response to Ultra-High Loading Rates, NRC Rept. NMAB-356 (1980).

9. Bai, Y.L., Thermo-Plastic Instability in Simple shear, J. Mech. Phys. Sol. 30 (1982) 195-207.

10. Pan, J., Perturbation Analysis of Shear Strain Localization in Rate Sensitive Materials, Int. J. Solids and Structures 19 (1983) 153-164.

11. Burns, T.J. and Trucano, T.G., Instability in Simple Shear Deformations of Strain Softening Materials, Mech. Mat. 1 (1982) 313-324.

12. Burns, T.J., Approximate Linear Stability Analysis of a Model of Adaiabatic Shear Band Formation, SAND83-1907 (Oct. 1983) Sandia National Laboratories, Albuquerque, NM 87185; Quart. Appl. Math. 43 (1985) 65-84.

Nonlinear Calculations of Shear Band Formation

13. Merzer, A.M., Modeling of Adiabatic Shear Band Development from Small Imperfections, J. Mech. Phys. Sol. 30 (1983) 323-338.

14. Clifton, R.J., Duffy, J., Hartley, K.A., and Shawki, T.G., On Critical Conditions for Shear Band Formation at High Strain Rates, Scripta Met. 18 (1984) 443-448 (see also Shawki, Clifton, Majda, Analysis of Shear Strain Localization in Thermal Visco-Plastic Materials, Brown Univ. Report ARO DAAG29-81-K-0121/3 Oct. 1983).

15. Wu, F.H. and Freund, L.B., Deformation Trapping Due to Thermoplastic Instability in One-Dimensional Wave Propagation, J. Mech. Phys. Sol. 32 (1984) 119-132.

16. Wright, T.W. and Batra, R.C., The Initiation and Growth of Adiabatic Shear Bands, Int. J. Plasticity 1 (1985) 205-212.

17. Wright, T.W. and Batra, R.C., Further Results on the Initiation and Growth of Adiabatic Shear Bands at High Strain Rates, J. de Physique, Coll. C5, suppl. to 468 (1985).

Continuum Model with Distributed Shear Bands

18. Seaman, L., Curran, D.R., and Shockey, D.H., Scaling of Shear Band Fracture Processes, Sagamore 29, 295-307 (see also Erlich, Seaman, Shockey and Curran, Development and Application of a Computational Shear Band Model, Stanford Research Institute DAAD05-76-C-0762 (1977)).

Viscoplasticity

19. Cristescu, N., Dynamic Plasticity, North Holland, Amsterdam (1967).

20. Perzyna, P., Thermodynamic theory of Viscoplasticity, Advances in Applied Mechanics 11 (1971) 313-354.

21. Malvern, L.E., Experimental and Theoretical Approaches to Characterization of Material Behavior at High Rates of Deformation, in Mechanical Properties at High Rates of Strain, Proc. 3rd Oxford Conf. 1984, ed. J. Harding, Inst. Phys., London (1984) 1-20.

Bifurcation Theory

22. Budiansky, B., Theory of Buckling and Post-Buckling Behavior of Elastic Structures, Adv. Appl. Mech. 14, ed. C.-S. Yih, Academic Press, New York (1974) 2-66.

23. Hutchinson, J.W., Plastic Buckling, Adv. Appl. Mech. 14, ed. C.-S. Yih, Academic Press, New York (1974) 67-145.

24. Iooss, G. and Joseph, D.D., Elementary Stability and Bifurcation Theory, Springer-Verlag, New York (1980).

25. Serrin, J., On the Stability of Viscous Fluid Motions, Arch. Rat. Mech. Anal. 3 (1959) 1-13.

26. Neitzel, G.P. and Davis, S.H., Energy Stability Theory of Decelerating Swirl Flows, Phys. Fluids 23 (1980) 432-437.

Simplification and Complexification

27. Varley, E., private communication (1985).

28. Green, A.E., McInnis, B.C., and Naghdi, P.M., Elastic-Plastic Continua with Simple Force Dipole, Int. J. Eng. Sci. 6 (1968) 373-394.

DISTRIBUTION LIST

No. of Copies	Organization
12	Administrator Defense Technical Info Center ATTN: DDC-DDA Cameron Station Alexandria, VA 22304-6145
4	Director Defense Advanced Research Projects Agency ATTN: Tech Info Dr. E. Van Reuth Dr. G. Farnum Dr. B. Wilcox 1400 Wilson Boulevard Arlington, VA 22209
1	Deputy Assistant Secretary of the Army (R&D) Department of the Army Washington, DC 20310
1	HQDA DAMA-ART-M Washington, DC 20310
1	Commander US Army War College ATTN: Lib Carlisle Barracks, PA 17013
1	Commander US Army Command and General Staff College ATTN: Archives Fort Leavenworth, KS 66027
1	Commander US Army Materiel Command ATTN: AMCDRA-ST 5001 Eisenhower Avenue Alexandria, VA 22333-0001
1	Commander Armament R&D Center US Army AMCCOM ATTN: SMCAR-LCA, T. Davidson Dover, NJ 07801-5001
3	Commander Armament R&D Center US Army AMCCOM ATTN: SMCAR-SC, J. D. Corrie J. Beetle E. Bloore Dover, NJ 07801-5001
1	Commander Armament R&D Center US Army AMCCOM ATTN: SMCAR-TDC Dover, NJ 07801-5001
1	Commander Armament R&D Center US Army AMCCOM ATTN: SMCAR-TSS Dover, NJ 07801-5001
1	Commander Benet Weapons Laboratory ATTN: Dr. E. Schneider Watervliet, NY 12189
1	Director Benet Weapons Laboratory Armament R&D Center US Army AMCCOM ATTN: SMCAR-LCB-TL Watervliet, NY 12189
1	Commander US Army Armament, Munitions and Chemical Command ATTN: SMCAR-ESP-L Rock Island, IL 61299-7300
1	Commander US Army Aviation Research and Development Command ATTN: AMSAV-E 4300 Goodfellow Boulevard St. Louis, MO 63120

DISTRIBUTION LIST

No. of Copies	Organization
1	Director US Army Air Mobility Research and Development Command Ames Research Center Moffett Field, CA 94035
1	Commander US Army Communications - Electronics Command ATTN: AMSEL-ED Fort Monmouth, NJ 07703-5301
1	Commander US Army Electronics Research and Development Command Technical Support Activity ATTN: DELSD-L Fort Monmouth, NJ 07703-5301
1	Commander US Army Harry Diamond Laboratory ATTN: SLCHD-TA-L 2800 Powder Mill Road Adelphi, MD 20783
1	Commander MICOM Research, Development and Engineering Center ATTN: AMSMI-RD Redstone Arsenal, AL 35898-5500
1	Director Missile and Space Intelligence Center ATTN: AIAM-S-YDL Redstone Arsenal, AL 35898-5500
3	Director BMD Advanced Technology Center ATTN: ATC-T, M. Capps ATC-M, S. Brockway ATC-RN, P. Boyd P.O. Box 1500 Huntsville, AL 35807
2	Commander US Army Mobility Equipment Research & Development Command ATTN: DRDME-WC DRSME-RZT Fort Belvoir, VA 22060
1	Commander US Army Natick Research and Development Center ATTN: DRXRE, Dr. D. Sieling Natick, MA 01762
1	Commander US Army Tank Automotive Command ATTN: AMSTA-TSL Warren, MI 48397-5000
1	Commander USAG ATTN: Technical Library Fort Huachuca, AZ 85613-6000
1	Commander US Army Development and Employment Agency ATTN: MODE-TED-SAB Fort Lewis, WA 98433
3	Commander US Army Laboratory Command Materials Technology Laboratory ATTN: SLCMT-T, J. Mescall SLCMT-T, R. Shea SLCMT-H, S.C. Chou Watertown, MA 02172-0001
1	Director US Army TRADOC Systems Analysis Activity ATTN: ATAA-SL White Sands Missile Range, 88002

DISTRIBUTION LIST

No. of Copies	Organization
1	Commandant US Army Infantry School ATTN: ATSH-CD-CSO-OR Fort Benning, GA 31905
1	Director US Army Advanced BMD Technology Center ATTN: CRDABH-5, W. Loomis P. O. Box 1500, West Station Huntsville, AL 35807
3	Commander US Army Research Office ATTN: Dr. E. Saibel Dr. G. Mayer Dr. J. Chandra P. O. Box 12211 Research Triangle Park, NC 27709
2	Commander US Army Research and Standardization Group (Europe) ATTN: Dr. J. Wu Dr. F. Oertel Box 65 FPO NY 09510
3	Office of Naval Research Department of the Navy ATTN: Dr. Y. Rajapakse Dr. A. Tucker Dr. A. Kushner Washington, DC 20360
3	Commander US Naval Air Systems Command ATTN: AIR-604 Washington, DC 20360
1	Commander Naval Sea Systems Command ATTN: Code SEA 62D Department of the navy Washington, DC 20362-5101
3	Commander Naval Surface Weapons Center ATTN: Dr. W. H. Holt Dr. W. Mock Tech Lib Dahlgren, VA 22448-5000
3	Commander Naval Surface Weapons Center ATTN: Dr. R. Crowe Code R32, Dr. S. Fishman Code X211, Lib Silver Spring, MD 20902-5000
1	Commander and Director US Naval Electronics Laboratory San Diego, CA 92152
5	Air Force Armament Laboratory ATTN: AFATL/DLODL J. Foster John Collins Joe Smith Guy Spitale Eglin AFB, FL 32542-5000
1	RADC (EMTLD, Lib) Griffiss AFB, NY 13440
1	AUL (3T-AUL-60-118) Maxwell AFB, AL 36112
1	Air Force Wright Aeronautical Laboratories Air Force Systems Command Materials Laboratory ATTN: Dr. Theodore Nicholas Wright-Patterson AFB, OH 45433

DISTRIBUTION LIST

No. of Copies	Organization
1	Air Force Wright Aeronautical Laboratories Air Force Systems Command Materials Laboratory ATTN: Dr. John P. Henderson Wright-Patterson AFB, OH 45433
1	Director Environmental Science Service Administration US Department of Commerce Boulder, CO 80302
1	Director Lawrence Livermore Laboratory ATTN: Dr. M. L. Wilkins P. O. Box 808 Livermore, CA 94550
9	Sandia National Laboratories ATTN: Dr. L. Davison Dr. P. Chen Dr. L. Bertholf Dr. W. Herrmann Dr. J. Nunziato Dr. S. Passman Dr. E. Dunn Dr. T. Burns Dr. M. Forrestal P. O. Box 5800 Albuquerque, NM 87185-5800
1	Sandia National Laboratories ATTN: Dr. D. Bamman Livermore, CA 94550
1	Director National Aeronautics and Space Administration Lyndon B. Johnson Space Center ATTN: Lib Houston, TX 77058
1	Director Jet Propulsion Laboratory ATTN: Lib (TDS) 4800 Oak Grove Drive Pasadena, CA 91103
1	A.R.A.P. Group, Titan Systems, Inc. ATTN: Ray Gogolewski 1800 Old Meadow Rd., #114 McLean, VA 22102
1	ETA Corporation ATTN: Dr. D. L. Mykkanen P. O. Box 6625 Orange, CA 92667
1	Forestal Research Center Aeronautical Engineering Lab. Princeton University ATTN: Dr. A. Eringen Princeton, NJ 08540
1	Honeywell, Inc. Defense Systems Division ATTN: Dr. Gordon Johnson 600 Second street, NE Hopkins, MN 55343
2	Orlando Technology, Inc. ATTN: Dr. Daniel Matuska Dr. John J. Osborn P. O. Box 855 Shalimar, FL 32579
6	SRI International ATTN: Dr. Donald R. Curran Dr. Donald A. Shockey Dr. Lynn Seaman Mr. D. Erlich Dr. A. Florence Dr. R. Caligiuri 333 Ravenswood Avenue Menlo Park, CA 94025

DISTRIBUTION LIST

No. of Copies	Organization
1	Systems Planning Corporation ATTN: Mr. T. Hafer 1500 Wilson Boulevard Arlington, VA 22209
1	Terra-Tek, Inc. ATTN: Dr. Arfon Jones 420 Wahara Way University Research Park Salk Lake City, UT 84108
2	California Institute of Technology Division of Engineering and Applied Science ATTN: Dr. E. Sternberg Dr. J. Knowles Pasadena, CA 91102
1	Denver Research Institute University of Denver ATTN: Dr. R. Recht P. O. Box 10127 Denver, CO 80210
1	Massachusetts Institute of Technology ATTN: Dr. R. Probstein 77 Massachusetts Avenue Cambridge, MA 02139
1	Massachusetts Institute of Technology Department of Mechanical Engineering ATTN: Prof. L. Anand Cambridge, MA 02139
3	Rensselaer Polytechnic Institute ATTN: Prof. E. H. Lee Prof. E. Krempl Prof. J. Flaherty Troy, NY 12181
1	Southwest Research Institute Department of Mechanical Sciences ATTN: Dr. U. Lindholm 8500 Culebra Road San Antonio, TX 78228
5	Brown University Division of Engineering ATTN: Prof. R. Clifton Prof. H. Kolsky Prof. L. B. Freund Prof. A. Needleman Prof. R. Asaro Providence, RI 02912
1	Brown University Division of Applied Mathematics ATTN: Prof. C. Dafermos Providence, RI 02912
3	Carnegie-Mellon University Department of Mathematics ATTN: Dr. D. Owen Dr. M. E. Gurtin Dr. B. D. Coleman Pittsburgh, PA 15213
7	Cornell University Department of Theoretical and Applied Mechanics ATTN: Dr. Y. H. Pao Dr. G. S. S. Ludford Dr. A. Ruoff Dr. J. Jenkins Dr. R. Lance Dr. F. Moon Dr. E. Hart Ithaca, NY 14850
2	Harvard University Division of Engineering and Applied Physics ATTN: Prof. J. R. Rice Prof. J. Hutchinson Cambridge, MA 02138

DISTRIBUTION LIST

No. of Copies	Organization
2	Iowa State University Engineering Research Laboratory ATTN: Dr. A. Sedov Dr. G. Nariboli Ames, IA 50010
2	Lehigh University Center for the Application of Mathematics ATTN: Dr. E. Varley Dr. R. Rivlin Bethlehem, PA 18015
1	New York University Department of Mathematics ATTN: Dr. J. Keller University Heights New York, NY 10053
1	North Carolina State University Department of Civil Engineering ATTN: Prof. Y. Horie Raleigh, NC 27607
1	Pennsylvania State University Engineering Mechanical Dept. ATTN: Prof. N. Davids University Park, PA 16502
1	Rice University ATTN: Dr. C. C. Wang P. O. Box 1892 Houston, TX 77001
1	Southern Methodist University Solid Mechanics Division ATTN: Prof. H. Watson Dallas, TX 75221
1	Temple University College of Engineering Tech. ATTN: Dr. R. Haythornthwaite Dean Philadelphia, PA 19122
5	The Johns Hopkins University ATTN: Prof. R. B. Pond, Sr. Prof. R. Green Prof. W. Sharpe Prof. J. F. Bell Prof. C. A. Truesdell 34th and Charles Streets Baltimore, MD 21218
1	Tulane University Department of Mechanical Engineering ATTN: Dr. S. Cowin New Orleans, LA 70112
3	University of California Department of Mechanical Engineering ATTN: Dr. M. Carroll Dr. W. Goldsmith Dr. P. Naghdi Berkeley, CA 94704
1	University of California Dept of Aerospace and Mechanical Engineering Science ATTN: Dr. Y. C. Fung P. O. Box 109 La Jolla, CA 92037
1	University of California Department of Mechanics ATTN: Dr. R. Stern 504 Hilgard Avenue Los Angeles, CA 90024

DISTRIBUTION LIST

No. of Copies	Organization
1	University of California at Santa Barbara Department of Mechanical Engineering ATTN: Prof. T. P. Mitchel Santa Barbara, CA 93106
1	University of California at Santa Barbara Department of Materials Science ATTN: Prof. A. G. Evans Santa Barbara, CA 93106
1	University of California at San Diego Department of Mechanical Engineering ATTN: Prof. S. Nemat Nassar La Jolla, CA 92093
2	University of Delaware Department of Mechanical and Aerospace Engineering ATTN: Dr. Minoru Taya Prof. J. Vinson Newark, DE 19711
3	University of Florida Department of Engineering Science and Mechanics ATTN: Prof. L. Malvern Prof. D. Drucker Prof. E. Walsh Gainesville, FL 32601
2	University of Houston Department of Mechanical Engineering ATTN: Dr. T. Wheeler Dr. R. Nachlinger Houston, TX 77004
2	University of Illinois Department of Theoretical and Applied Mechanics ATTN: Dr. D. Carlson Prof. D. Scott Stewart Urbana, IL 61801
2	University of Illinois at Chicago Circle College of Engineering Department of Engineering, Mechanics, and Metallurgy ATTN: Prof. T.C.T. Ting Prof. D. Krajcinovic P. O. Box 4348 Chicago, IL 60680
2	University of Kentucky Department of Engineering Mechanics ATTN: Dr. M. Beatty Prof. O. Dillon, Jr. Lexington, KY 40506
1	University of Kentucky School of Engineering ATTN: Dean R. M. Bowen Lexington, KY 40506
2	University of Maryland Department of Mathematics ATTN: Prof. S. Antman Prof. T. P. Liu College Park, MD 20742
3	University of Minnesota Department of Engineering Mechanics ATTN: Prof. J. L. Erickson Prof. R. Fosdick Prof. R. James Minneapolis, MN 55455

DISTRIBUTION LIST

No. of Copies	Organization
1	University of Missouri-Rolla Department of Engineering Mechanics ATTN: Prof. R. C. Batra Rolla, MO 65401-0249
1	University of Pennsylvania Towne School of Civil and Mechanical Engineering ATTN: Prof. Z. Hashin Philadelphia, PA 19105
4	University of Texas Department of Engineering Mechanics ATTN: Dr. M. Stern Dr. M. Bedford Prof. Ripperger Dr. J. T. Oden Austin, TX 78712
1	University of Washington Department of Aeronautics and Astronautics ATTN: Dr. Ian M. Fyfe 206 Guggenheim Hall Seattle, WA 98195
1	University of Wyoming Department of Mathematics ATTN: Prof. R. E. Ewing P. O. Box 3036 University Station Laramie, WY 82070
3	Washington State University Department of Physics ATTN: Prof. R. Fowles Prof. G. Duvall Prof. Y. Gupta Pullman, WA 99163
2	Yale University ATTN: Dr. B.-T. Chu Dr. E. Onat 400 Temple Street New Haven, CT 96520
	Aberdeen Proving Ground
	Dir, USAMSAA ATTN: AMXSY-D AMXSY-MP, H. Cohen
	Cdr, USATECOM ATTN: AMSTE-TO-F
	Cdr, CRDC, AMCCOM ATTN: SMCCR-RSP-A SMCCR-MU SMCCR-SPS-IL

USER EVALUATION SHEET/CHANGE OF ADDRESS

This Laboratory undertakes a continuing effort to improve the quality of the reports it publishes. Your comments/answers to the items/questions below will aid us in our efforts.

1. BRL Report Number _____ Date of Report _____

2. Date Report Received _____

3. Does this report satisfy a need? (Comment on purpose, related project, or other area of interest for which the report will be used.) _____

_____

_____

4. How specifically, is the report being used? (Information source, design data, procedure, source of ideas, etc.) _____

_____

_____

5. Has the information in this report led to any quantitative savings as far as man-hours or dollars saved, operating costs avoided or efficiencies achieved, etc? If so, please elaborate. _____

_____

_____

6. General Comments. What do you think should be changed to improve future reports? (Indicate changes to organization, technical content, format, etc.)

_____

_____

_____

CURRENT ADDRESS

_____
Name

_____
Organization

_____
Address

_____
City, State, Zip

7. If indicating a Change of Address or Address Correction, please provide the New or Correct Address in Block 6 above and the Old or Incorrect address below.

OLD ADDRESS

_____
Name

_____
Organization

_____
Address

_____
City, State, Zip

(Remove this sheet along the perforation, fold as indicated, staple or tape closed, and mail.)

— — — — — — — — — FOLD HERE — — — — — — — — —

Director
U.S. Army Ballistic Research Laboratory
ATTN: SLCBR-DD-T
Aberdeen Proving Ground, MD 21005-5066

NO POSTAGE
NECESSARY
IF MAILED
IN THE
UNITED STATES

OFFICIAL BUSINESS
PENALTY FOR PRIVATE USE, $300

BUSINESS REPLY MAIL
FIRST CLASS PERMIT NO 12062 WASHINGTON, DC
POSTAGE WILL BE PAID BY DEPARTMENT OF THE ARMY

Director
U.S. Army Ballistic Research Laboratory
ATTN: SLCBR-DD-T
Aberdeen Proving Ground, MD 21005-9989

— — — — — — — — — FOLD HERE — — — — — — — — —